

## Study of deformation twinning and planar slip in a TWIP steel by Electron Channeling Contrast Imaging in a SEM

Ivan Gutierrez-Urrutia<sup>1,a</sup> and Dierk Raabe<sup>1,b</sup>

<sup>1</sup>Max-Planck-Institut für Eisenforschung GmbH, 40237 Düsseldorf, Germany

<sup>a</sup>i.gutierrez@mpie.de, <sup>b</sup>d.raabe@mpie.de

**Keywords:** Electron Channeling Contrast Imaging; EBSD; dislocation substructure; twin substructure; TWIP steel

**Abstract.** We study the dislocation and twin substructures in a high manganese twinning-induced-plasticity steel (TWIP) by means of electron channeling contrast imaging. At low strain (true strain below 0.1) the dislocation substructure shows strong orientation dependence. It consists of dislocation cells and planar dislocation arrangements. This dislocation substructure is replaced by a complex dislocation/twin substructure at high strain (true strain of 0.3-0.4). The twin substructure also shows strong orientation dependence. We identify three types of dislocation/twin substructures. Two of these substructures, those which are highly favorable or unfavorable oriented for twinning, exhibit a Schmid behavior. The other twin substructure does not fulfill Schmid's law.

### Introduction

Advanced metallic materials commonly exhibit several deformation mechanisms resulting in complicated deformed microstructures. High manganese steels represent a grade of advanced steels with high technological interest because of their outstanding mechanical properties, with a combination of high mechanical strength and ductility (ultimate tensile strength of 1 GPa and ductility to fracture of 50% [1]). These steels may exhibit several hardening mechanisms such as twinning induced plasticity (TWIP), transformation induced plasticity (TRIP) or micro-band induced plasticity (MBIP) resulting in complicated deformation microstructures. The activation of these mechanisms is strongly dependent on the stacking fault energy. The study of the corresponding dislocation and twin substructures is key to obtain a better understanding of strain hardening mechanisms and therefore, mechanical properties.

In particular, high manganese TWIP steels are characterized by a hierarchical microstructure refinement which includes complex dislocation and twin substructures, and their interactions [1, 2]. The twin substructure consists of bundles of several mechanical twins along  $\{111\} \langle 112 \rangle$  active twin systems. Concerning the dislocation substructure, some works have shown that high-Mn steels mainly contain a planar dislocation arrangement along  $\{111\}$  planes. This is attributed to the low stacking fault energy of these alloys (20-40 mJ/m<sup>2</sup>) [1].

The characterization of the deformed microstructure in high-Mn steels is a challenging task since it involves microstructure features at different length scales. As a consequence of this scale discrepancy, quantitative microstructure characterization by electron microscopy techniques such as electron backscatter diffraction (EBSD) or transmission electron microscopy (TEM) is limited due to the angular resolution (EBSD) and the small field of view (TEM), respectively. In this study, therefore, we make use of Electron Channeling Contrast Imaging (ECCI), which is conducted in the scanning electron microscope (SEM), to perform a quantitative characterization of the deformed microstructure of a TWIP steel.

### Experimental

The TWIP steel used in this study had the chemical composition Fe-22wt.% Mn-0.6wt.% C. Details of the processing route are described in [2]. The hot-rolled material showed a fully austenitic structure with an average grain size of 50 microns which remained stable during deformation at room temperature.

Tensile tests were carried out at room temperature at a strain rate of  $5 \times 10^{-4} \text{ s}^{-1}$  to different true strain levels. The monotonic tensile deformation experiments were carried out on a tensile test instrument Kammrath & Weiss GmbH (44141 Dortmund, Germany) equipped with a digital image correlation (DIC) system (ARAMIS system, GOM-Gesellschaft für Optische Messtechnik mbH, 38106 Braunschweig, Germany) to measure the local and macroscopic strain distribution. Details of this set-up are described in [3]. The surface pattern required for DIC was obtained as explained in [2]. Averaged engineering strain values were retrieved from the corresponding strain maps and used to calculate the true stress-strain values.

Microstructures of the tensile deformed TWIP steel were examined by two types of scanning electron microscopy techniques, namely, electron back scatter diffraction (EBSD) and electron channeling contrast imaging (ECCI). Orientation maps were performed in a 6500 F JEOL field emission gun-scanning electron microscope (FEG-SEM) equipped with a TSL OIM EBSD system at 15 kV acceleration voltage and a working distance of 15 mm. EBSD maps are displayed as inverse pole figure (IPF) maps in the direction of the tensile axis (TA) and shear direction (SD) for tensile and shear deformed samples, respectively. The ECCI technique was used to image deformation twins and dislocation substructures as introduced in previous works on TWIP steels [2, 4]. A new recently reported set-up for ECCI [5] was used in this study to obtain ECCI images under controlled diffraction conditions which enabled an enhanced dislocation and interface contrast. The set-up makes use of the EBSD technique for orienting the crystal into optimal diffraction conditions. ECCI images were obtained with optimum contrast by orienting the matrix crystal exactly in Bragg condition for a high intensity reflection and exciting the corresponding diffraction vector in a “two-beam” condition. The diffraction vector is depicted in each ECCI image. ECCI observations were carried out in a Zeiss Crossbeam instrument (XB 1540, Carl Zeiss SMT AG, Germany) consisting of a Gemini-type field emission gun (FEG) electron column and a focused ion beam (FIB) device (Orsay Physics). ECCI was performed at 10 kV acceleration voltage and a working distance of 6 mm, using a solid-state 4-quadrant BSE detector.

## Results and discussion

The ECCI technique has been established as an excellent tool in imaging microstructure features such as deformation twins, stacking faults, and complex dislocation arrangements at a wide field of view directly in the SEM [2, 5-8]. The reason of the recent maturation of the ECCI technique lies in its combination with EBSD. This allows us to efficiently identify optimum contrast conditions and, therefore, perform ECCI images of crystal defects under controlled diffraction conditions [5]. We study dislocation and twin substructures at two strain regimes according to the strain hardening behavior [4]: low strain (true strain below 0.1) and high strain (true strain of 0.3-0.4).

**Dislocation substructure.** At low strain (true strain below 0.1), the deformed microstructure is formed by a well-developed dislocation substructure. This substructure consists of dislocation cells with average size of 650 nm, Fig. 1(a), and planar dislocation structures, Fig. 1(b). This heterogeneous dislocation substructure is formed due to the multiple character of slip (planar and wavy). Planar slip character in fcc metals is known to be mainly promoted by decreasing stacking fault energy, increasing friction stress, and the occurrence of short range ordering [9, 10]. In the present TWIP steel, where ordering has not been observed, the two parameters that can promote planar slip are predominantly the friction stress and the stacking fault energy [4]. The latter effect promotes slip via Shockley partial dislocations. These can only cross slip after stress- and thermally assisted local recombination, hence the planar slip prevalence in materials with low stacking fault energy. The planar dislocation substructures shown in Fig. 1(b) are referred to as highly-dense dislocation walls (HDDWs) [11]. HDDWs are dislocation boundaries with a high dislocation density and a rotational component separating regions with different combinations of simultaneously operating glide systems. HDDWS have been observed in medium-high stacking

fault energy metals [11] as well as in low stacking fault energy alloys [12, 13]. Wavy dislocation structures, similar to that shown in Fig. 1(a), are promoted in grains when a high number of slip planes are activated and dislocation cross slip is enabled [11, 14]. These substructures are commonly observed in medium-to-high stacking fault energy metals [11].

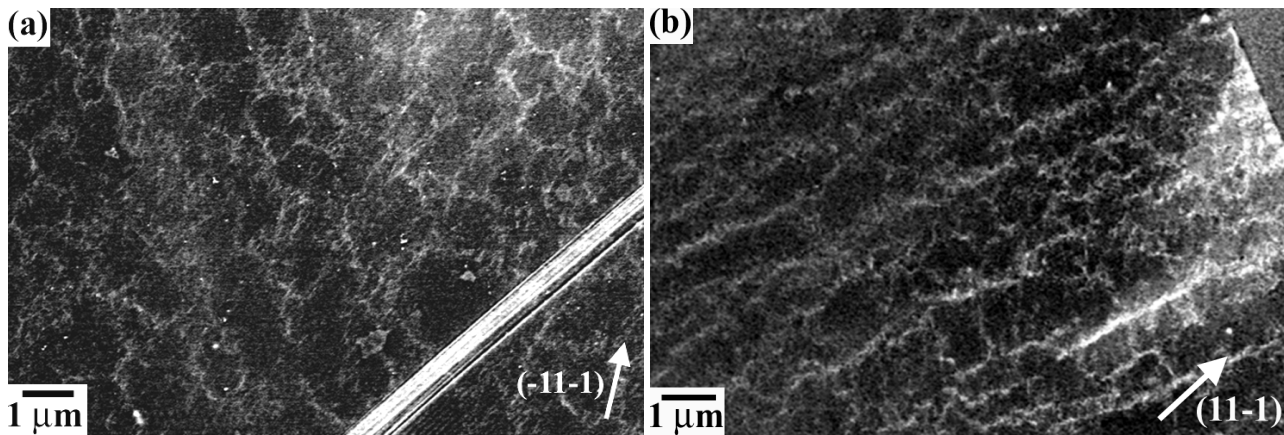


Fig. 1. ECCI images of dislocation cell structure (a) and planar dislocation arrangements (b) in tensile deformed TWIP steel to 0.1 true strain.

Fig. 2 shows the TA-IPF at 0.1 true strain. Although at this strain level the texture is weak, it can be seen that the texture is characterized by a  $\langle 001 \rangle$ - $\langle 111 \rangle$  fiber. We observe a strong orientation dependence of dislocation substructure. Dislocation cells are observed in grains oriented close to  $\langle 001 \rangle // TA$  and planar dislocation arrangements in grains oriented within the region close to the pole  $\langle 111 \rangle // TA$ .

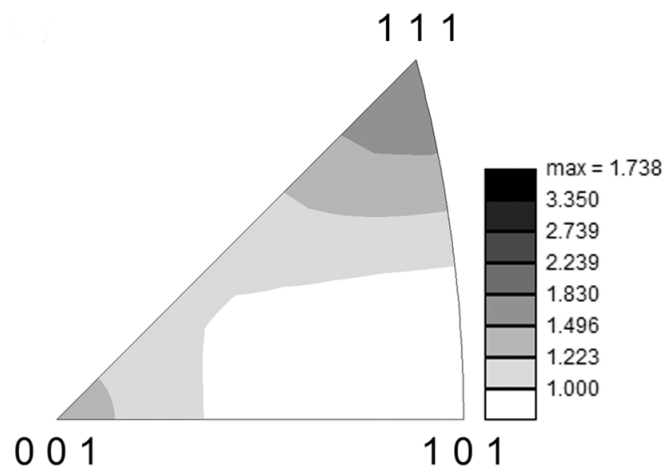


Fig. 2. Inverse pole figure along the tensile axis of tensile deformed TWIP steel to 0.1 true strain.

Interestingly, a similar crystallographic orientation dependence of the dislocation substructure as observed for the current Fe-Mn alloy has been reported in medium-to-high stacking fault energy metals such as Cu-3at%Al alloy [15] and pure aluminum [16]. The formation of an equiaxed cell structure is a common feature of grains in a polycrystal oriented close to  $\langle 001 \rangle // TA$  direction in high-to-medium stacking fault energy metals. This is ascribed to the easy activation of multiple-slip (four to eight slip systems have high and similar Schmid factors). However, there is another aspect that must be considered in cell formation, which is dislocation cross-slip. This mechanism plays an important role in the cell formation through the re-arrangement of screw dislocations in terms of the activation of secondary slip and annihilation of screw dislocations of opposite sign. The localized maneuvers of partial dislocations to transfer dislocation screw segments from one plane to another

depends on the stacking fault energy [17]. As the present Fe-Mn contains a low stacking fault energy ( $22 \text{ mJ/m}^2$  [18]), dislocation cross-slip is not a favorable mechanism. This result suggests that for the present Fe-Mn alloy, the mechanism of dislocation cell formation may be different to that occurring in medium-high stacking fault energy metals. The formation of planar dislocation arrangements in grains close to  $\langle 111 \rangle // \text{TA}$  direction indicates that there are two active slip systems in the same slip plane that account for a large fraction of the total slip in the respective crystal [19].

**Twinning substructure.** At high strain (true strain of 0.3-0.4), the deformed microstructure consists of a dislocation and twinning substructure. This substructure is strongly dependent on the crystallographic orientation. Fig. 3 shows the TA-IPF at 0.4 true strain. At this strain level, the texture is characterized by a sharp  $\langle 001 \rangle$ - $\langle 111 \rangle$  fiber.

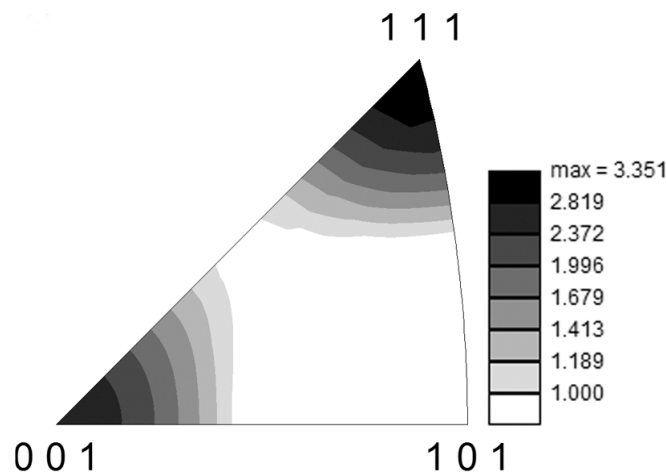


Fig. 3. Inverse pole figure along the tensile axis of tensile deformed TWIP steel to 0.4 true strain (a).

At this strain regime, we can identify three types of deformed substructures: Type I, II and III, fig. 4. Type I corresponds to grains that are oriented close to  $\langle 001 \rangle // \text{TA}$  directions and exhibit low deformation twinning activity and a well-developed dislocation cell structure. Type II grains are oriented along the line between the  $\langle 001 \rangle // \text{TA}$  and  $\langle 111 \rangle // \text{TA}$  crystallographic directions and contain a lamellar twin structure along a primary twinning system. Twin boundaries cut through the existing dislocation substructure developed at low strain (planar dislocation structures and dislocation cells) without experiencing strong resistance. As a consequence, the dislocation substructure is removed and replaced by a new block-shaped nanostructure. This nanostructure consists of twin boundaries along the twin system and dislocation boundaries formed along the most active slip systems. Type III grains are oriented close to  $\langle 111 \rangle // \text{TA}$  directions and exhibit a significant deformation twinning and dislocation activity. The twinning activity results in a well-defined twin substructure consisting of a primary twin system and one or two secondary twin systems. We define primary twin system as the system with the highest Schmid factor for twinning. The other twin systems are referred as to secondary twin systems. As in Type II grains, twin boundaries cut through the existing dislocation substructure. However, in these grains the twin substructure does not completely remove the former dislocation substructure. Accordingly, a rhomboid-shaped nanostructure of twin boundaries and dislocation boundaries is formed. The evolution of this nanostructure is further favored by twin-twin intersections due to the activation of multiple twin systems.

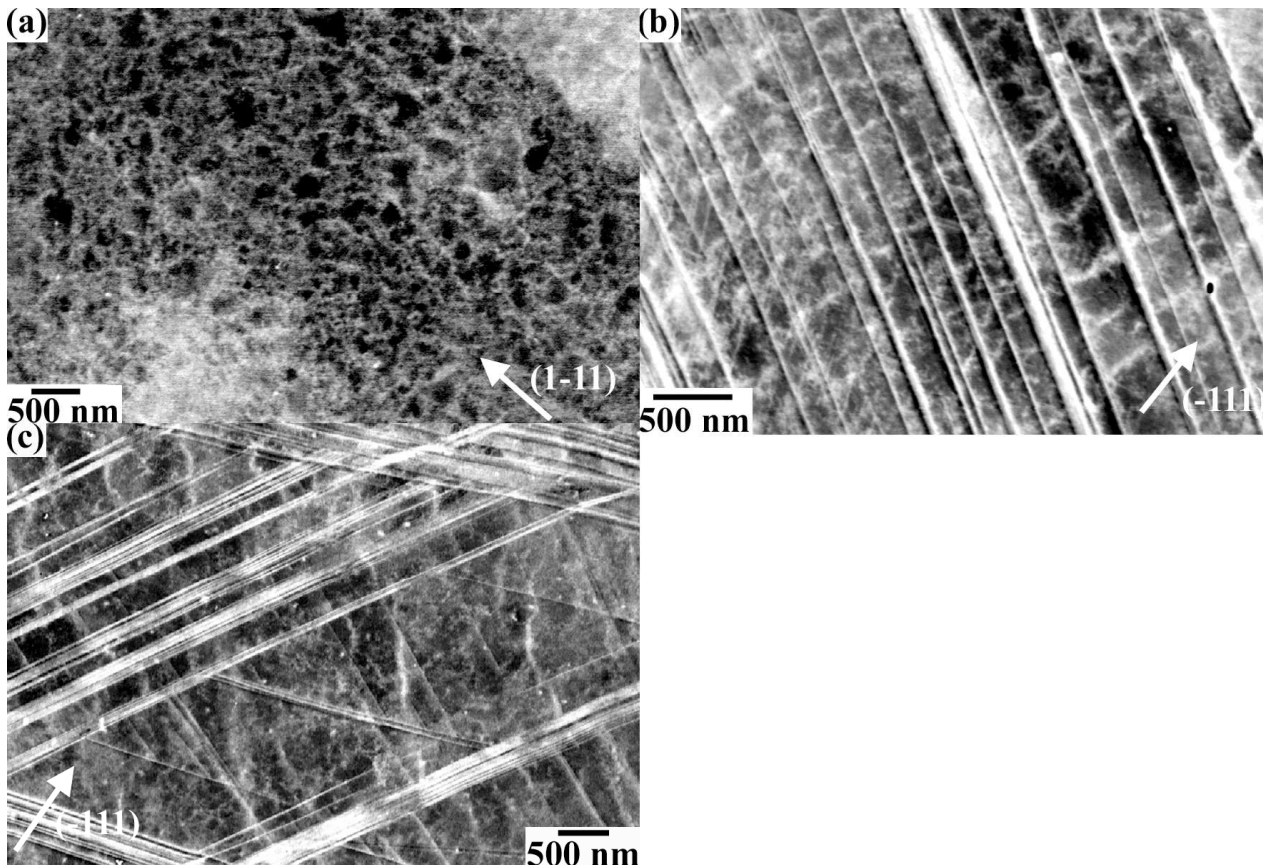


Fig. 4. ECCI images of Type I (a), Type II (b) and Type III (c) grains. Type I grains are oriented close to  $\langle 001 \rangle // \text{TA}$  directions, Type II along the line  $\langle 001 \rangle - \langle 111 \rangle$  and Type III close to  $\langle 111 \rangle // \text{TA}$  directions. TA: tensile axis. Type I, II, and III grains are described in the text.

Fig. 5(a) shows the orientation dependence of the deformed microstructure on 150 grains analyzed by means of ECCI and EBSD. Fig. 5(b) shows the corresponding orientation dependence of deformation twinning for the present tensile deformed fcc metal. In this figure,  $m_{\text{tw}}$  and  $m_{\text{slip}}$  are the Schmid factor for twinning and slip, respectively. Accordingly, if we assume a Schmid behavior on both twinning and slip, the region with  $m_{\text{tw}} > m_{\text{slip}}$  is favorable oriented for deformation twinning and the region with  $m_{\text{tw}} < m_{\text{slip}}$  is favorable oriented for slip. The observed twin substructure cannot be fully explained in terms of Schmid's law with respect to the macroscopic stress state. Only grains with a highly favorable (Type III grains) or unfavorable (Type I grains) orientation for twinning follow the Schmid behavior. Type II grains, which contain a lamellar twin structure, follow a non-Schmid behavior. Furthermore, some deviations from the Schmid behavior are observed even in Type I grains. Small twins (few microns in length) nucleated at grain boundaries are commonly observed in these grains. These deviations from Schmid behavior are ascribed to local stress concentrations at grain boundaries (for example, provided by the impingement of deformation twins formed in a neighboring grain on a grain boundary) that can promote twinning in unfavorable oriented grains for twinning with respect to the macroscopic stress state, i.e. Type I and most of Type II grains. In particular, the developed twin substructure in Type II grains may hinder the growth of deformation twins on secondary twin systems because the stress required to build up a secondary twin substructure is probably too high to be attained during tensile deformation. As a consequence, the primary twin system is triggered resulting in a lamellar twin structure. This effect is similar to the well known effect of overshooting in slip due to latent hardening.

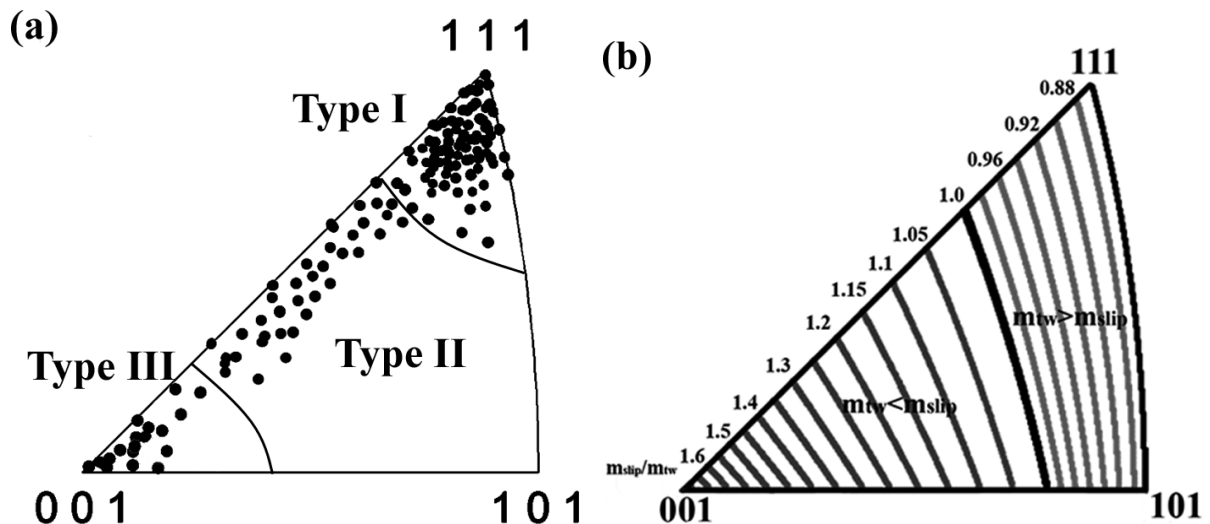


Fig. 5. (a): Orientation dependence of twin substructures Type I, II and III. (b): Orientation dependence of twinning and slip according to Schmid's law in a tensile deformed fcc metal.  $m_{tw}$  and  $m_{slip}$  are Schmid factor for twinning and slip, respectively.

## Summary

We study dislocation and twin substructures in a FeMnC TWIP steel by means of electron channeling contrast. At low strain (true strain below 0.1) the dislocation substructure shows strong crystallographic orientation dependence. It consists of dislocation cells and planar dislocation arrangements. At high strain (true strain of 0.3-0.4) the former dislocation substructure is replaced by a complex dislocation/twin substructure. This substructure also shows strong crystallographic orientation dependence. We identify three types of dislocation/twin substructures. Two of these substructures, viz. Type I and III, which are highly unfavourable and favourable oriented for twinning, respectively, mainly exhibit a Schmid behavior. The other twin substructure, namely, Type II crystals, does not fulfill Schmid's law.

## Acknowledgments

The authors would like to acknowledge the financial support by the German Research Foundation (Deutsche Forschungsgemeinschaft DFG) within the framework of the SFB 761 "steel ab initio".

## References

- [1] O. Bouaziz, S. Allain, C.P. Scott, P. Cugy, D. Barbier, High manganese austenitic twinning induced plasticity steels: A review of the microstructure properties, *Current Opinion Solid State Mater. Sci.* in press (2011).
- [2] I. Gutierrez-Urrutia, S. Zaefferer, D. Raabe, The effect of grain size and grain orientation on deformation twinning in a Fe-22 wt.% Mn-0.6 wt.% C TWIP steel, *Mater. Sci. Eng. A* 527 (2010) 3552-3560.
- [3] D. Raabe, M. Sachtler, Z. Zhao, F. Roters, S. Zaefferer, Micromechanical and macromechanical effects in grain scale polycrystal plasticity. Experimentation and simulation, *Acta Mater.* 49 (2001) 3433-3441.
- [4] I. Gutierrez-Urrutia, D. Raabe: submitted to *Acta Materialia* (2011)

- 
- [5] I. Gutierrez-Urrutia, S. Zaeferrer, D. Raabe, Electron channeling contrast imaging of twins and dislocations in twinning-induced plasticity steels under controlled diffraction conditions in a scanning electron microscope, *Scripta Mater.* 61 (2009) 737-740.
- [6] A.J. Wilkinson, P.B. Hirsch, Electron diffraction based techniques in scanning electron microscopy of bulk materials, *Micron* 28 (1997) 279-308.
- [7] M.A. Crimp, Scanning Electron Microscopy Imaging of Dislocations in Bulk Materials, Using Electron Channeling Contrast, *Microscopy Research Technique* 69 (2006) 374-381.
- [8] A. Weidner, S. Martin, V. Klemm, U. Martin, H. Biermann, Stacking faults in high-alloyed metastable austenitic cast steel observed by electron channelling contrast imaging, *Scripta Mater.* 64 (2011) 513-516.
- [9] V. Gerold, H.P. Karnthaler, On the origin of planar slip in F.C.C. alloys, *Acta Metall.* 37 (1989) 2177-2183.
- [10] S.I. Hong, C. Laird, Mechanisms of slip mode modifications in f.c.c. solid solutions, *Acta Mater.* 38 (1990) 1581-1594.
- [11] B. Bay, N. Hansen, D.A. Hughes, D. Kuhlmann-Wilsdorf, Overview N° 96. Evolution of F.C.C. deformation structures in polyslip, *Acta Metall. Mater.* 40 (1992) 205-219.
- [12] D. Canadinc, H. Sehitoglu, H.J. Maier, Y.I. Chumlyakov, Strain hardening behavior of aluminum alloyed Hadfield steel single crystals, *Acta Mater.* 53 (2005) 1831-1842.
- [13] D. Canadinc, H. Sehitoglu, H.J. Maier, The role of dense dislocation walls on the deformation response of aluminum alloyed hadfield steel polycrystals, *Mater. Sci. Eng. A* 454-455 (2007) 662-666.
- [14] D. Kuhlmann-Wilsdorf, Theory of plastic deformation:-properties of low energy dislocation structures, *Mater. Sci. Eng. A* 113 (1989) 1-41.
- [15] T. Mori, H. Fujita, Effect of dislocation structure on the flow stress in Cu-3at.%Al single crystals, *Phil. Mag. A* 46 (1982) 91-104.
- [16] N. Hansen, X. Huang, Microstructure and flow stress of polycrystals and single crystals, *Acta Mater.* 46 (1998) 1827-1836.
- [17] J.P. Hirth, J. Lothe, *Theory of dislocations*, John Wiley & Sons, 1982.
- [18] L. Bracke, L. Kestens, J. Penning, Direct observation of the twinning mechanism in an austenitic Fe–Mn–C steel, *Scripta Mater.* 61 (2009) 220-222.
- [19] G. Winther, D. J. Jensen, N. Hansen, Dense dislocations walls and microbands aligned with slip planes. Theoretical considerations, *Acta Mater.* 45 (1997) 5059-5068.